SYNTHESIS AND CHARACTERISATION OF NANO TITANIA MODIFIED WITH CARBON COMPOSITES AND ITS PHOTOCATALYTIC APPLICATION ON POLLUTION CONTROL

A MINOR RESEARCH PROJECT (XII PLAN)

SUBMITTED TO UGC

BY

Dr. RAJESH K. M.

ASSISTANT PROFESSOR DEPARTMENT OF CHEMISTRY

M. P. MOOTHEDATH SREE NARAYANA TRUSTS COLLEGE, SHORANUR

PALAKKAD, 679122, KERALA

(AFFILIATED TO CALICUT UNIVERSITY)

Synthesis and Characterisation of Nano Titania Modified with Carbon Composites and its Photocatalytic Application on Pollution Control

Introduction

Titania is the one of the most common semiconductor used in the area of photocatalysis due to its fascinating properties such as strong oxidizing power, non toxicity, long-term photostability, biological and chemical inertness [1,2]. Upon on irradiation of titania with energy equal to or greater than its bandgap (3.2eV), the electrons move to the conduction band (CB) to generate positive holes in the valence band (VB). The positive holes can react with adsorbed H_2O to form hydroxyl radicals while the electrons react with O_2 to form superoxide radicals. Being highly reactive, the OH and O_2 radicals can oxidize the pollutants in solution or react with adsorbed pollutants [3].

Due to the rapid recombination of photo induced electron/hole pair and narrow light response range based on its band gap, titania suffers a main drawback as its low photocatalytic efficiency in visible region [1, 4-11]. In order to improve the photocatalytic efficiency, many approaches are introduced by various research group such as increasing the adsorption abilities of the photocatalyst surface by adding a co-adsorbent [1,12] doping with metal, non metals or semiconductor to improve the separation between free carriers and brings its activity in visible region of electromagnetic spectrum [13,14].

Graphene (new allotrope of carbon) is a two-dimensional honeycomb lattice of sp^2 carbon atoms with high electronic, thermal, optical and mechanical properties [1,15,16] has attracted by scientists since its discovery in 2004 by Geim et. al.[17, 18]. Since there is a small overlap between the valence and conduction bands, and graphene exhibits semimetal behavior [3]. It is a 0 eV bandgap semiconductor [19] with high mobility of charge carriers [20], high specific surface area ($\sim 2600 m^2 g^{-1}$) [21] and a high adsorption capacity.

Various methods have been reported in literature for the preparation of graphene and are generally classified as bottom-up and top-down approaches. The bottom-up approaches involve the direct synthesis of graphene from carbon sources, such as chemical vapour deposition, epitaxial growth etc. but they are not used widely because of their complexity. The common top-down methods such as micromechanical exfoliation, chemical exfoliation of graphite, mechanical exfoliation, thermal exfoliation, electrostatic deposition, chemical and electrochemical reduction of graphite oxide etc [2,22-30]. Among these methods, the reduction of exfoliated graphene oxide (GO) was proven to be an effective and reliable method to produce graphene with low cost and high stability. The exfoliated GO provides oxygen-containing functional groups, such as carboxylic, hydroxyl, and epoxide, which allows interactions with the cations and provides reactive sites for the nucleation and growth of nano particles, results in the rapid growth of various graphene-based composites. Moreover, the functional GO can be reduced to graphene with partial restoration of the sp^2hybridized network by various reduction methods [15].

The surface properties of graphene can be adjusted via chemical modification, which offers tremendous opportunities for the development of functionalized graphene-based materials and are applied in the field of energy storage, fuel cells, chemical detectors, solar cells, catalysis, biosensors, molecular imaging, nano electronics, intercalation materials, super capacitors, polymer composites and drug delivery [3,15,17,31-37]. Due to its extra ordinary properties, it received tremendous increased attention in the field of the photocatalytic efficiency of semiconductors [38-41]. In graphene-based composites, graphene acts either as a functional component or a substrate for immobilizing the other components. The electronic properties of GO and reduced GO have been reported that it reducing the carrier recombination and increasing light absorption range of titania photocatalyst and hence enhances the photocatalytic ability, which giving significant advantages to using GO/reduced GO as support structures [42-44].

There are numerous attempts have been made to combine graphene with titania semiconductor photocatalysts to enhance their photocatalytic performance. The widely used preparation methods are in situ growth, simple colloidal blending method, self-assembly solution mixing, hydrothermal and/or solvothermal method, electrochemical deposition, atomic layer deposition,

electron beam irradiation, sol-gel, ultra sonication etc [3,14,15,30,44-49]. Each method has its own merits and demerits such as most of them were based on a complicated and lengthy experimental procedure for synthesis, which limited their practical applications.

The sol−gel processing method is one of the most common procedure, which allows compositional and micro structural tailoring through controlling the precursor chemistry and processing conditions to produce nano composite photo catalysts; which also possible to control a number of determining parameters of the final product such as homogeneity, purity, and microstructure (in particular porosity and surface area). Furthermore, the sol−gel approach provides excellent chemical homogeneity and the possibility of deriving unique meta stable structures at low reaction temperatures [17, 50,51].

In this study, we highlighted the synthesis and characterization of TiO_2 –graphene composite through sol-gel methods and evaluate its photocatalytic activity using the degradation studies of aqueous methlylene blue dye solution in solar light irradiation. We also compare the phtocatalytic degradation studies of methylene blue dye solution with TiO_2 – graphene composite prepared by sonication and hydrothermal methods (their characterization techniques are not mentioned). A modified Hummer method was used for the preparation of graphene.

Experimental and Characterisation

Materials: The chemicals used in this study were purchased from various manufactures with specification as shown below. Graphite powder, Con. Sulphuric acid, Phosphoric acid, Potassium permanganate, Con. Hydrochloric acid, Hydrogen peroxide, Hydrazine hydrate, Ethanol, Deionized water, Cetyltrimethylammonium bromide (CTAB), Titanium tetraisopropoxide (TTIP), Triethanolamine, Isopropyl alcohol. Unless otherwise specified, all the reagents and materials involved were used as received without further purification

Preparation of Catalyst:

Synthesis of Graphene oxide (GO): Go was synthesized by modified Hummers methods [14, 52,53] in which a 9:1 H_2SO_4 and H_3PO_4 solution was prepared. For this 360 ml con. H_2SO_4 was taken in 1L beaker and placed in a magnetic stirrer. To this add 40 ml H_3PO_4 drop wise with

stirring. Add 3g graphite powder slowly to the mixture in the stirrer. Now add 18g $KMnO_4$ slowing to this mixture and maintain the temperature of mixture below 50^0C and stirrer for 12 hours. Pour the mixture to 400 ml ice water along with 27 ml 30% H_2O_2. Mix well. Centrifuge the mixture using micro centrifuge and washed three times with 1M HCl and 3 times with deionized water. Finally it was filtered using 0.2micron filter paper placed in glass filter assembly with suction pump to get light brown powder.

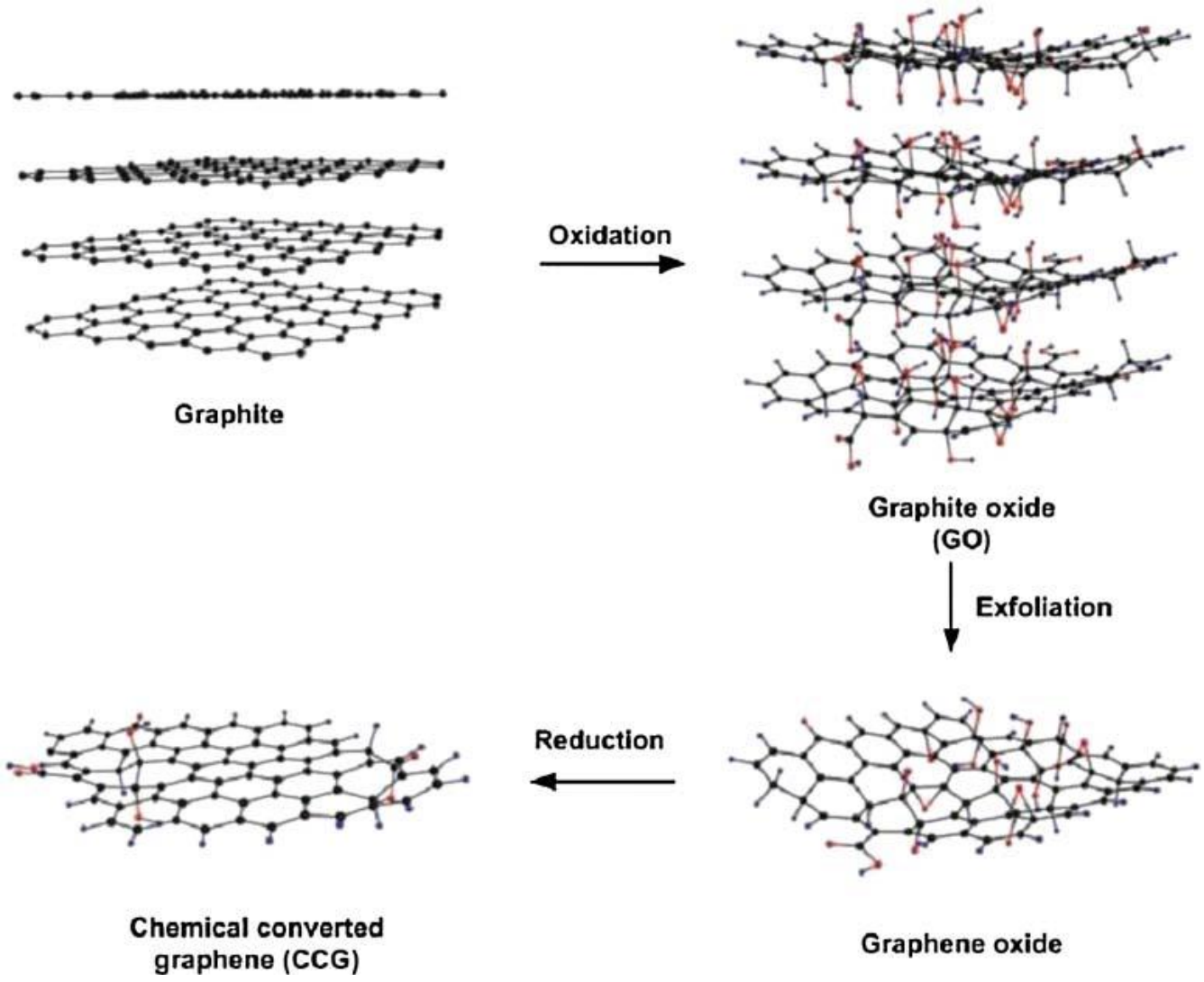

Synthesis of Reduced Graphene oxide (RGO):100 mg of the above prepared GO was taken in 250ml beaker and add around 100 ml deionized water. This solution is sonicated for 2 hours giving a yellow brown dispersion. It is then reduced to graphene by adding 1 ml Hydrazine

hydrate and the solution was heated at 80^0C for 16 hour. The reduced GO then gradually precipitated as black solid which then separated by filtration, washed with ethanol and deionzed water and dried at 80 ^{0}C.

Preparation of Graphene-Titania composite[G-TiO_2(SG)]: 0.08g of the RGO, 0.5g of cetyl trimethylammonium bromide (CTAB) and 25 ml ethanol were taken in 100 beaker and stirred magnetically for about 30 min. To this add 11 ml titanium tetraisopropoxide dropwise with stirring. Add 20 ml deionized water dropwise to the mixer and the suspension was stirred for 8 hours to get sol and dried at 60^0C to get gel. The above gel was calcined in a muffle furnace at 500 ^{0}C for 10 min and naturally cooled down to room temperature. The obtained product was grinded well and labeled as G-TiO_2(SG). Pure tiatania was also prepared in the same method except the addition of RGO and the product was labeled as TiO_2.

We also prepared two other Graphene-Titania composite through Sonication and hydrothermal method. In sonication method [1], we avoid the calcinations treatment and the product was labeled as G-TiO_2(S) and in hydrothermal method [3], the product was labeled as G-TiO_2(HT). In both case we use GO and Titanium tetraisopropoxide as precursor for C and Ti. (In present study we did not carried out any characterization studies of these two catalysts. But we use these catalysts for comparison of photocatalytic studies with graphene-titania composite prepared through sol-gel method).

Characterisation:

The X-ray diffraction (XRD) patterns were recorded using *Bruker* AXS D8 advance X ray Diffractometer with Ni filtered Cu Kα radiation(λ = 0.15406 nm). The intensities were obtained in the 2θ range 20 - 70 ^{0}. The crystallite size was determined from the broadening of the major peak in the XRD spectrum using the Scherrer equation, $D = K \lambda / \beta \cos\theta$. Where D is the crystallite size, K = 0.9 is a constant, λ is the X-ray wavelength, β is full width half maximum of the major peak and θ is the diffraction angle. The Diffuse Reflectance UV-Visible spectra of the powder samples were recorded in the range of 200-800 nm on a Varian, Cary 5000 UV-Visible NIR spectrophotometer. The FTIR spectra were recorded in Thermo Nicolet, Avatar 370 FTIR Spectrometer by means of KBr pellet procedure. Spectra were taken in the transmission mode

under atmospheric pressure and room temperature. The changes in the absorption bands were investigated in the 400-4000 cm^{-1} range. The resolution and acquisition applied were 4 cm^{-1} and 60 scans respectively. The Transmission Electron Microscopy (TEM) images were recorded *Jeol* JEM 2100 ultrahigh resolution analytical electron microscope with operating voltage 20-200kV and resolution point 0.23 nm, lattice 0.14nm. A sonicated solution of the sample in alcohol, which evaporates on the TEM grid to form a dry film, was prepared. X-ray photoelectron microscopy (XPS) using ESCA+, (omicron nanotechnology, Oxford Instrument Germany) equipped with monochromator Aluminum Source (Al ka radiation hv =1486.7ev). The instrument was operated at 15 kv and 20mA. Pass energy [for short scan pass energy is 20ev and in case of survey it was 50ev]. Sample were taken in powder from / pellet form, and deposited on Cu tape and degassed for overnight in XPS FEL chamber to minimize the air contaminator at sample surface as well as degasing in main chamber. To overcome the charging problem a charge neutralizer of 2 keV is applied and binding energy of C1s core (284.6ev) was taken as reference.

Photocatalytic studies:

The experiments were carried using direct sun light in the time period of 10.30 am to 3.30 pm on hot days. Studies involve a 10 ml of 10^{-4} M aqueous methylene blue dye solution taken in beaker to this add the catalyst and stirred for 30 minute to achieve the adsorption equilibrium before the irradiation with sunlight. After the irradiation, the sample was taken out, centrifuged to remove the catalyst particles and properly diluted to measure its absorbance/ concentrations at wavelength of 653 nm using Visible Spectrophotometer (Elico). From which its percent of degradation is calculated. The experiments were repeated twice and its average was reported. Studies involve the change in amount of catalyst; kinetics and comparison with other catalysts were conducted

The percent of degradation is calculated as follows: Percent of Degradation = **{Co – C} x 100 / Co**. Where Co and C are the concentration of sample before and after irradiation

Results and Discussions

X-ray Diffraction Analysis (XRD):

Figure 1 a and b represents the XRD spectra of G-TiO_2(SG) and TiO_2. The peaks at $2\theta = 25.5^0$, 38.1^0, 48.2^0, 54.3^0, 55.1^0, 62.9^0 are attributed to the crystal planes (101),(114),(200),(211),(204) of anatase phase respectively [1,14, 54]. The absence of the peaks at $2\theta = 27.5^0$ and 30.8^0 indicates that the rutile and brookite phases are not present. There was no peak in the XRD spectrum that can be attributed to graphene. This is may due to low graphene content in the catalysts, or its low diffraction intensity (below the detection limit of the instrument) which results in the shielding of the graphne peaks by those of titania. [2,55-57]. The crystallite size calculated using Debye Scherrer equation for G-TiO_2(SG) and TiO_2 from 101 plane of anatase phase was 8.85 nm and 9.2 nm respectively. The smaller value of crystallite size of the graphene-titania composite compared to pure titania indicates that the incorporation of graphene into the titania system. The incorporation of graphene was also shown by slightly broadened the peak width of G-TiO_2(SG) when compared with TiO_2. It may be due to the interaction between titania and graphne during the hydrolysis of the sol samples. [40].

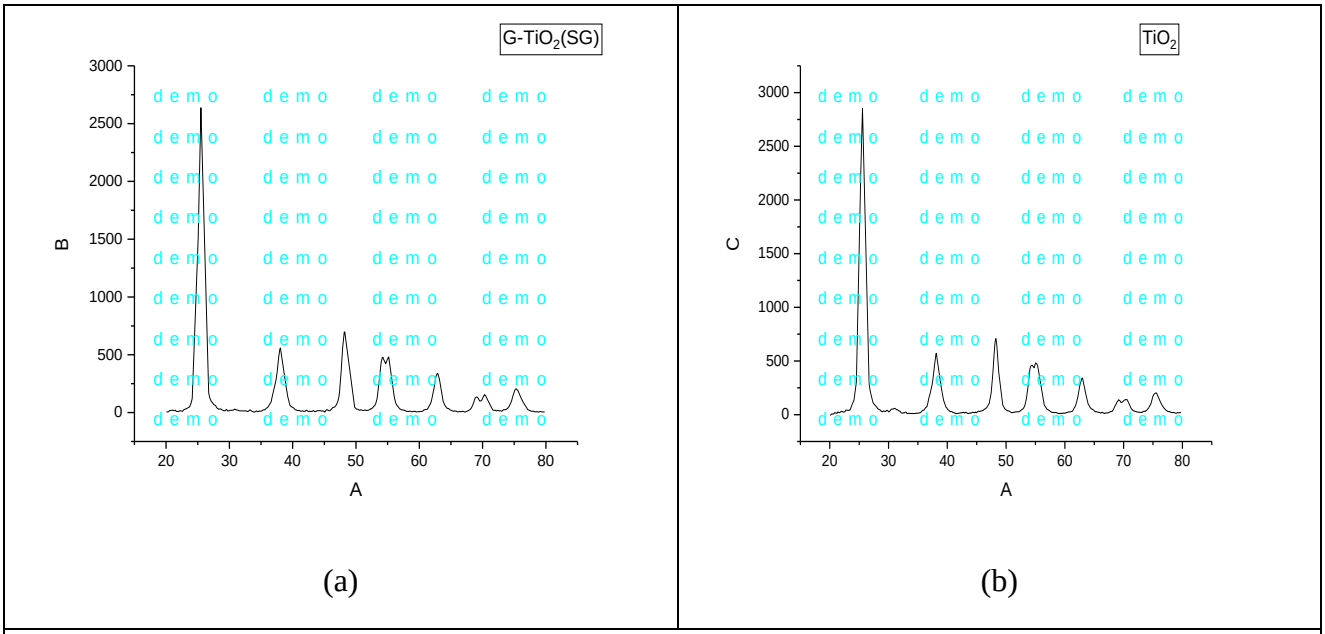

(a) (b)

Fig 1a and b : XRD spectra of G-TiO_2(SG) and TiO_2

Infrared Spectra Analysis:

Figure 2 a and b represents the FTIR spectra of G-TiO_2(SG) and TiO_2. Both spectra showed a broad band around 500-700 cm^{-1} and 3400-3420 cm^{-1} attributed to the Ti–O–Ti stretching and bending vibrational modes and O–H stretching frequency from the surface hydroxyl group respectively. Another major peak around 1625 cm^{-1} corresponds to hydroxyl group of molecular water [2]. There are some others very weak shoulder present G-TiO_2(SG) at 1170 cm^{-1}, 1500 cm^{-1}1720-1740 cm^{-1}, 1590-1620 $cm^{-1}$and 1620 cm^{-1} corresponding to C-OH stretching, skeletal vibration of graphene sheets, C=O stretching, C=C stretching and Ti-O-C stretching respectively. But these peaks are very very low intensity and not properly seen in full scan spectrum and many of them merged with peak of surface adsorbed hydroxyl goups[1,2,14,29]

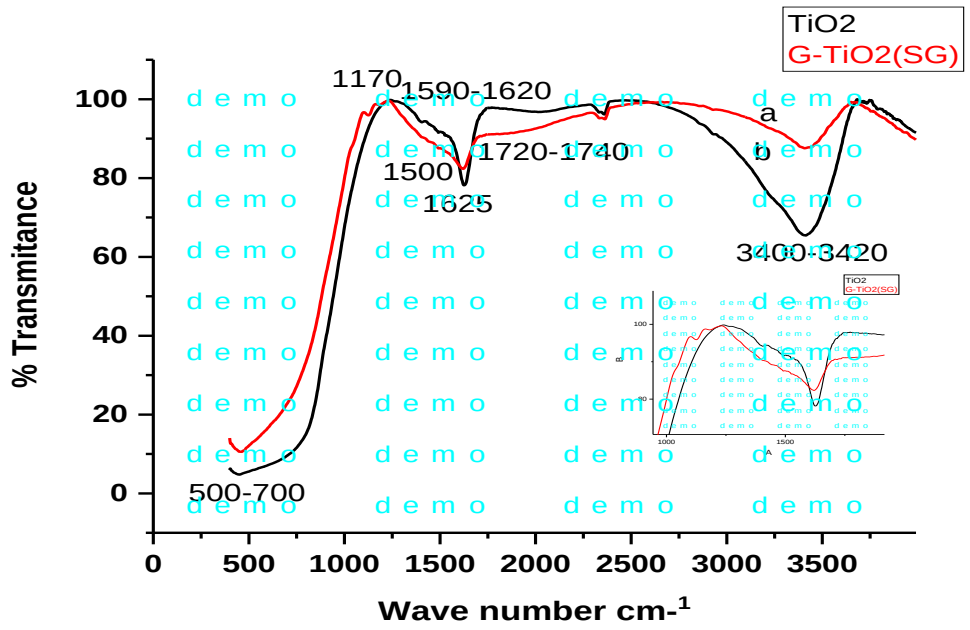

Fig. 2 a and b: IR spectra of G-TiO_2(SG) and TiO_2

UV-Visible Diffuse Reflectance Spectroscopy

Figure 3 showed the UV Visible Diffuse Reflectance spectra of the G-TiO_2(SG) and TiO_2. The spetra shows that the absorption edge of graphene-titania sample extended to visible region when compared to pure titania. But the intensity of light absorption in visible region is not much increased. Thus incorporation of graphene indicated that the interaction between graphene and titania. The introduction of graphene into the titania matrix effectively promote solar light response of the composite which attributed to electronic interactions between titania and graphne[2]. The shift in absorption edge may be attributed to the Ti-O-C bonds from hydrolysis of Ti precursor during sol gel process, which built new molecular orbital and narrow the band gap [14, 58, 59].

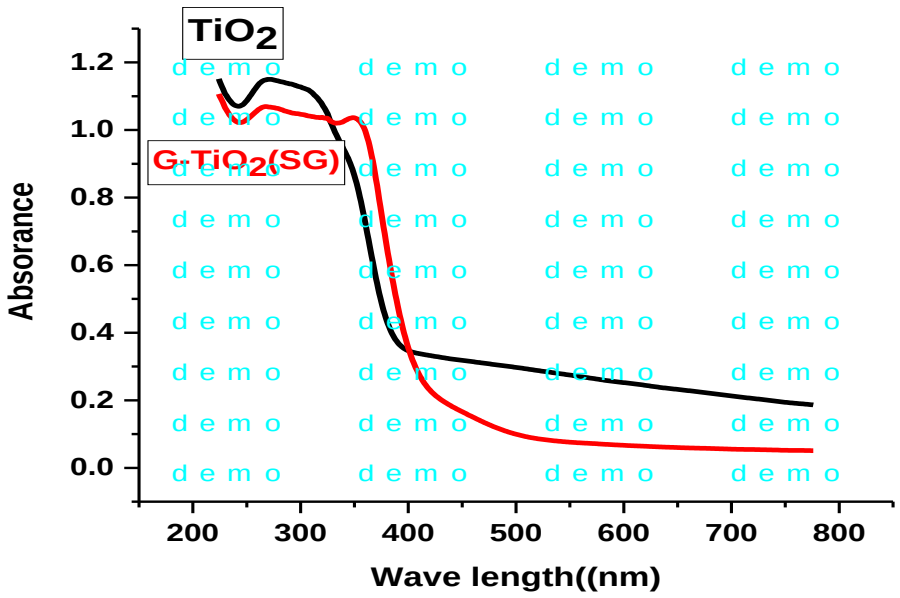

Fig.3: UV-Vis. DRS spectra of G-TiO_2(SG) and TiO_2

Transmission Electron Microscopy (TEM)

Fig. 4(a-d) Shows the TEM, HRTEM and SAED images of G-TiO_2(SG). Fig. 4(a) and (b) shows the TEM images. It can be clear from the picture that the titania nano particles are distributed on graphene sheets. Graphene sheets are clearly seen in fig 4(b). Also it was illustrated that the majority of the titania particles appeared spherical morphology with around 7-13 nm in size and homogeneously dispersed. But in some portions the particles are agglomerated. Thus sol-gel route facilitates interaction of functionalized graphene sheets with titania nano particles through its hydrolysis and poly condensation mechanism. The HRTEM and SAED fig.4(c) and 4(d) images clearly indicated that the graphen titania nano composite in which the titania nano particles are highly crystalline and ordered morphology. This was very much in agreement with XRD results.

X-ray Photoelectron Spectroscopy (XPS)

Fig. 5 (a-d) shows the XPS spectra of G-TiO_2(SG). Fig. 5 a shows the XPS survey scan spetra. Fig.5b. showed the C 1s peaks. The peak at 284.1 eV arises from elemental carbon, which corresponds to the adventitious carbon adsorbed on the surface of sample, where as peaks at 287.2, values suggest the presence of a carbonate species [6, 16,29,59-61].

Fig. 5 c. represents the Ti 2p core level photoelectron spectrum. The peaks at binding energies of 458.1 eV and 464.1 eV attributed to the Ti2p3/2 and Ti2p1/2 peaks, which is consistent with the value of Ti^{+4} in the TiO_2 lattice [6,16]. Fig. 5 d represents O 1s core levels. The main peaks at 529.1eV represents O in Ti-O of titania network and peaks at 531.8 eV due to the O of surface adsorbed hydroxyl group in titania [6]. Thus all the elements present in the graphene titania composite are confirmed.

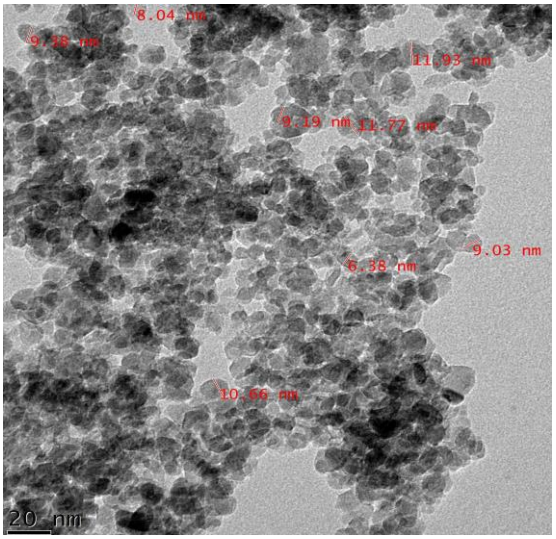

(a)

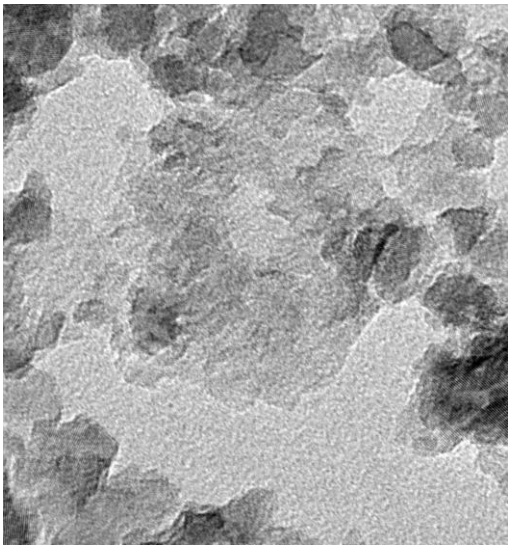

(b)

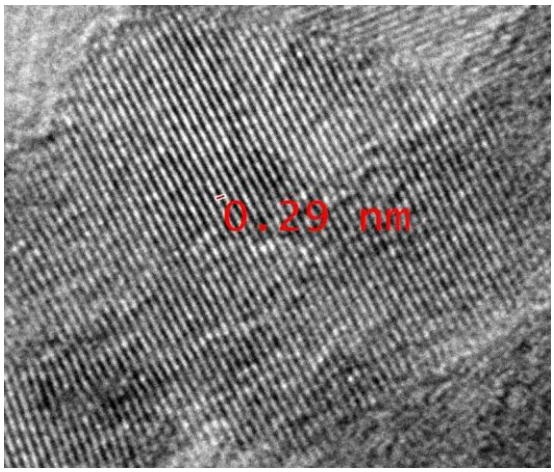

(c)

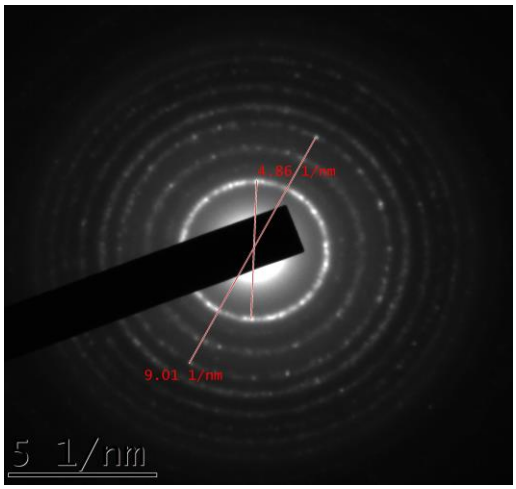

(d)

Fig 4.(a) and (b) TEM images, (c) HRTEM and (D)SAED of G-TiO2(SG)

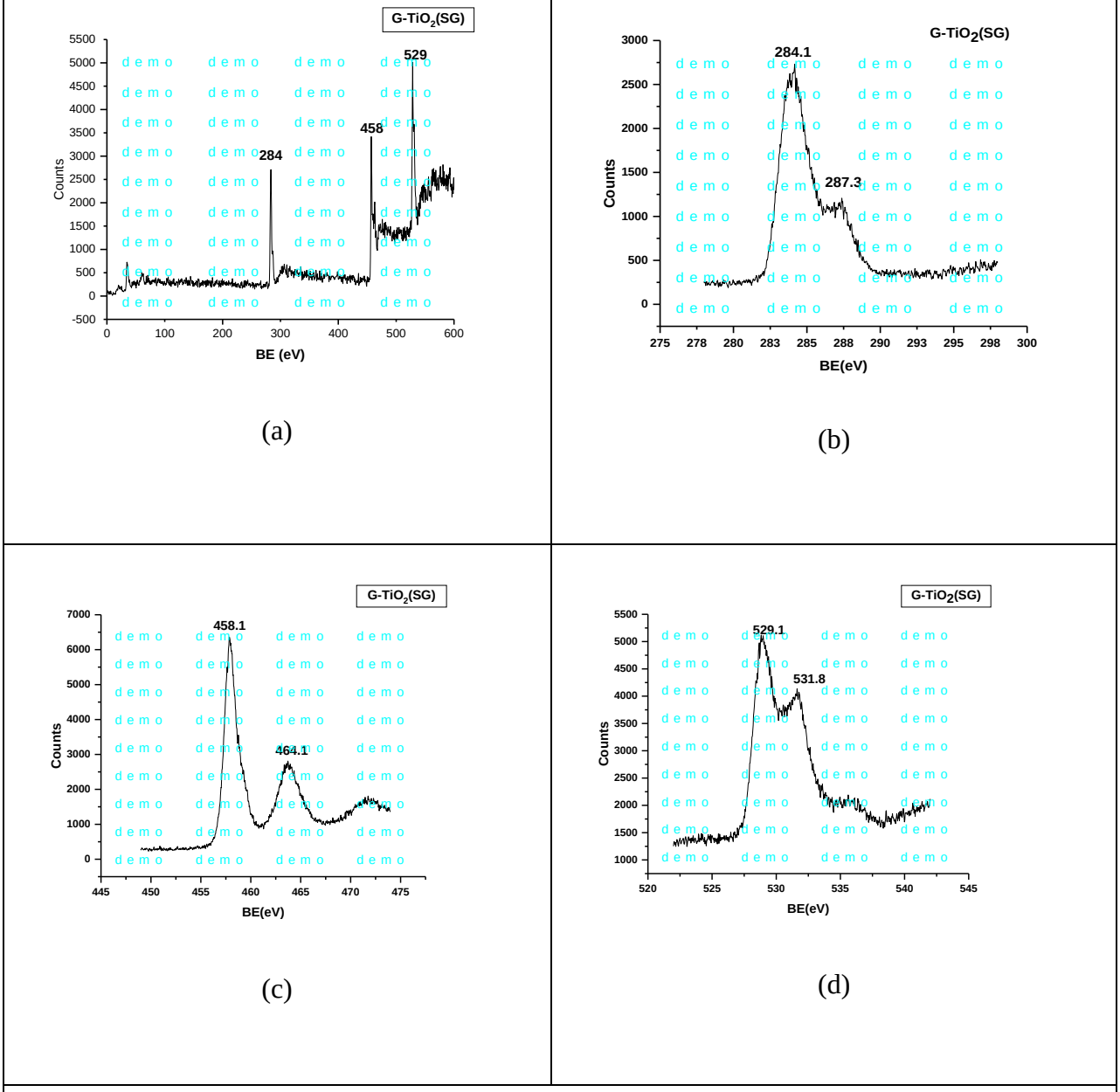

Fig 5.(a) survey scan (b) C 1s, (c) Ti 2p and (D)O 1s XPS spectra of G-TiO_2(SG)

Photocatalytic activity

Methylene blue is a aromatic heterocyclic dye compound. It has molecular formula $C_{16}H_{18}N_3SCl$. It is a dark green, odourless solid at room, which yields a blue solution when

dissolved in water and gives characteristic spectrophotometric absorbance at 635 nm. Methylene Blue (MB) is a cationic dye, extensively used in textile and coir industries commonly for coloring cotton, wood, paper stocks, and silk. It is also utilized in the field of medicine.

Severe exposure to methylene blue releases aromatic amines (e.g., benzidine, methylene) and is a potential carcinogen, it will cause increased heart rate, vomiting, shock, cyanosis, and tissue necrosis in humans due to these critical negative effects, methylene blue should be eliminated from the human environment. Its presence, even in very low concentration, is highly visible and will affect aquatic life as well as food web. In water, it causes to increase the BOD level and make it harmful for aquatic life. [61,62]

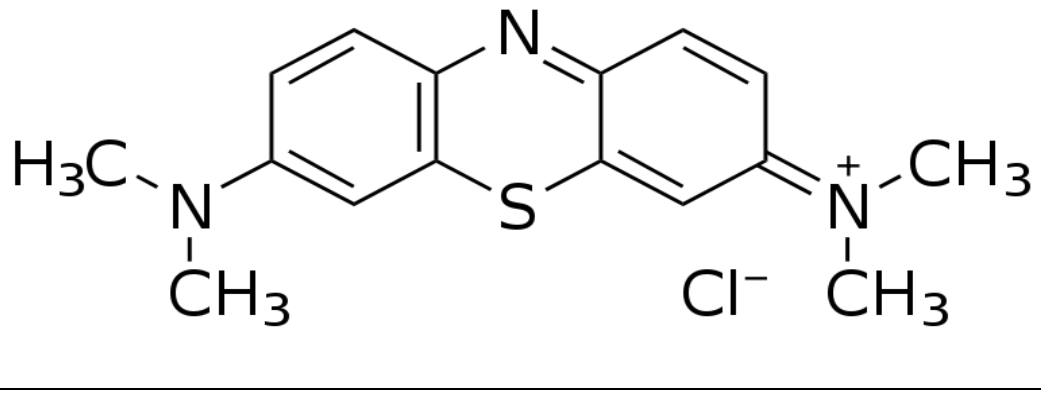

Fig. 6 a. Structure of methylene blue

Effect of amount of catalyst

Fig. 6 b. represent the effect of amount of catalyst of G-TiO_2(SG) against the photocatalytic degradation of methylene blue dye solution. From the figure it was clear the percent degradation increases with increase amount of catalyst concentration and reach a optimum value (around 90%) at 3 g/L. Above this limit there was not much increase in degradation. The increase of percent degradation with increase of catalyst amount may be due to the increase in the active sites available on the catalyst surface for the reaction and increase of light absorption consequently. However, at higher loadings, beyond the optimum, the rate of degradation is reduced due to light scattering and reduction in the light penetration through the solution. With a

higher catalyst loading the deactivation of activated molecules by collision with ground state molecules dominates the reaction, thus reducing the rate of reaction.

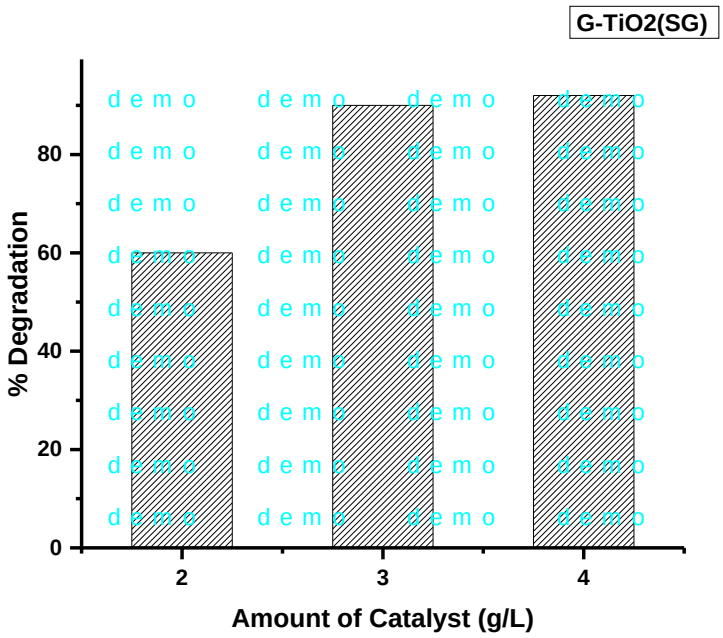

Fig. 6 b. % Degradation of methylene blue against amount of catalyst
Irradiation time: I hour; Dye con. 10 ml of 10^{-4} M

Effect of time

Fig. 6 c. represents the percent degradation of methylene blue dye against irradiation time. Study involved a 50 ml of 10^{-4} molar aqueous solution of methylene blue with catalyst amount of 3 g/L added, which is optimized by the above experiment. Before irradiation the system was magnetically stirred for 30 minutes under dark to establish the adsorption-desorption equilibrium between the catalytic surface and the dye. After the solution is irradiated with sun light, around 10ml of the suspension is pipette from the solution at an interval of 15 minutes. The pipetted sample is filtered and measured it absorbance

From the results it was noted that the modified catalysts G-TiO_2(SG) gives a linear increase of percentage of degradation with the increase time. The increase of degradation is assumed that

when time increases more and more light energy is fall on the catalyst surfaces which increases the formation of photo excited species and enhance the photocatalytic activity

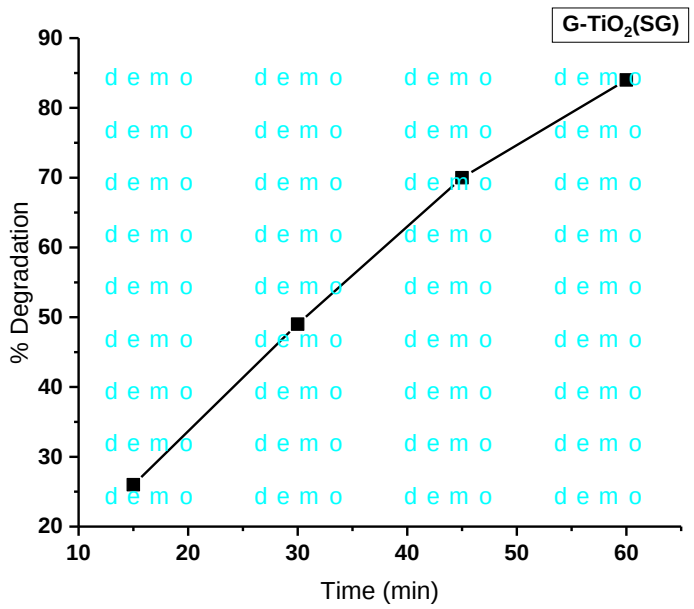

Fig. 6 c. % Degradation of methylene blue against irradiation time
Amount of Catalyst: 3 g/L; Dye con. 50 ml of 10^{-4} M

Effect of various catalyst

Table 6.1. represent the percent degradation of methylene blue against different catalyst. (The characterizations of other catalysts are not mentioned here). The table showed that the catalyst G-TiO_2(SG) gives better results compared to other catalyst. The higher degradation of G-TiO_2(SG) when compared with pure titania indicated the effect of graphene incorporation. Moreover the higher percent degradation of graphene titania composite through sol –gel method (G-TiO_2(S)) compared to that prepared through sonication method (G-TiO_2(SG)) and hydrothermal (G-TiO_2(HT)) method showed the advantage of sol –gel method over others. It was also well established that the catalytic action is specific

Catalyst	% of degradation
G-TiO_2(SG)	90
TiO_2	40
G-TiO_2(S)	58
G-TiO_2(HT)	65

Table 6 .1.. % Degradation of methylene blue against various catalyst
Irradiation time: 1 hour; Dye con. : 10 ml of 10^{-4} M, Catalyst: 3 g/L

.

Conclusion:

We are successful to synthesis nano crystalline graphene-titania composite through sol-gel method. Graphene was prepared through modified Hummer methods. The XRD results showed that the modified catalyst has purely anatase phase. The broadening of peak area indicated its highly crystalline nature. The crystalline nature with high ordered arrangement of particles was confirmed by HRTEM and SAED analysis. The anatase phase with main peaks at 101 plane also confirmed with XRD, HRTEM and SAED analysis. The crystallite size obtained from XRD shows very good agreement with the particle size obtained from TEM analysis. The IR spectrum indicated the presence of C peaks which very well correlated with the results obtained with XPS analysis. The shift in absorption edge into visible region confirm the reduction of band gap which results the high percent degradation of organic aqueous pollutant methylene blue (10 ml 10^{-4} M) solution when irradiated with sunlight with an optimum catalyst amount of 3 g/L.

Reference

1. Application of Titanium Dioxide-Graphene Composite Material For Photocatalytic Degradation of Alkylphenols: Chanbasha Basheer, Journal of Chemistry, Volume 2013, Article ID 456586,10 pages http://dx.doi.org/10.1155/2013/456586.

2. A green approach to the fabrication of titania–graphene nano composites: Insights relevant to efficient photodegradation of AcidOrange 7 dye under solar irradiation: P.Muthirulann,

C.Nirmala Devi, M.MeenakshiSundaram, Materials Science in Semiconductor Processing 25(2014)219–230.

3. Facile hydrothermal preparation of titanium dioxide decorated reduced graphene oxide nanocomposite: Betty Yea Sze Chang, Nay Ming Huang, Mohd Nor An'amt, Abdul Rahman Marlinda, Yusoff Norazriena, Muhamad Rasat Muhamad, Ian Harrison, Hong Ngee Lim, Chin Hua Chia, Int J Nanomedicine. 2012; 7: 3379–3387.

4. Increase of the photocatalytic activity of TiO_2 by carbon and iron modifications: B. Tryba International Journal of Photoenergy,vol.2008, ArticleID721824,15pages,2008.

5. Tuning the Photocatalytic Activity and Optical Properties of Mesoporous TiO_2 Spheres by a Carbon Scaffold: Leticia F. Velasco, Marta Haro, Julien Parmentier, Roger Gadiou, Cathie Vix-Guterl, Conchi O. Ania1. Journal of Catalysts Volume 2013, Article ID 178512, 9 pages. http://dx.doi.org/10.1155/2013/178512.

6. Enhanced photocatalytic activity of graphen-TiO_2 composite under visible light irradiation: N. R. Khalid, E. Ahmed, Zhanglian Hong, L. Sana, M. Ahmed. Current Applied Physics 13 (2013) 659-663.

7. Preparation and photocatalytic activity of rare earth doped TiO_2nanoparticles. V. Stengl, S. Bakardjieva, N. Murafa, Mater. Chem. Phys. 114 (2009) 217-226.

8. Visible-light photocatalysis in nitrogen-doped titanium oxides: R. Asahi, T. Morikawa, T. Ohwaki, K. Aoki, Y. Taga, J. Sci. 293 (2001) 269-271.

9. Heterogeneous photocatalysis: fundamentals and applications to the removal of various types of aqueous pollutants: J.M. Herrmann, Catal. Today 53 (1999) 115.

10. Origin of Photocatalytic Activity of Nitrogen-Doped TiO_2 Nanobelts: J. Wang, D.N. Tafen, J.P. Lewis, Z. Hong, A. Manivannan, M. Zhi, L. Ming, N.Q. Wu, J. Am. Chem. Soc. 131 (2009). 12290-12227.

11. Visible light photocatalytic activity in nitrogen-doped TiO_2 nanobelts: D. Tafen, J. Wang, N.Q. Wu, J.P. Lewis, Appl. Phys. Lett. 94 (2009) 093101.

12. Photocatalytic degradation of 4-nnonylphenol under irradiation from solar simulator: comparison between $BiVO_4$andTiO_2 photocatalysts: S.Kohtani, S.Makino, A.Kudo, K.Tokumura, Y.Ishigaki, Chemistry Letters, no.7,pp.660–661,2002.

13. Enhancement of adsorption and photocatalytic activity of TiO_2 by using carbon nanotubes for the treatment of azo dye: Y. Yu, J. C. Yu, C. Y. Chan et al.,Applied Catalysis B, vol. 61, no. 1-2,pp.1–11,2005.

14. Graphene facilitated visible light photo degradation of methylene blue over titanium dioxide photocatalysts: Shizhen Liu, Hongqi Sun, Shaomin Liu, Shaobin Wang, Chemical Engineering Journal 214 (2013) 298–303

15. Graphene-based semiconductor photocatalysts: Quanjun Xiang, Jiaguo Yu, Mietek Jaroniec, Received 24th June 2011 DOI: 10.1039/c1cs15172j.Chem. Soc. Rev.

16. Graphene/TiO_2 nanocomposites: synthesis, characterization and application in hydrogen evolution from water photocatalytic splitting: Xiao-Yan Zhang, Hao-Peng Li, Xiao-Li Cui, Yuehe Linb. J. Mater. Chem., 2010, 20, 2801–2806 | 2801

17. Synthesis of Fullerene, Carbon Nanotube and Graphene−TiO_2 Nanocomposite Photocatalysts for Selective Oxidation: A Comparative Study: Min-Quan Yang, Nan Zhang, and Yi-Jun Xu,. dx.doi.org/10.1021/am3029798. ACS Appl. Mater. Interfaces 2013, 5, 1156−1164.

18. Electric field effect in atomically thin carbon films: Novoselov, K. S.; Geim, A. K.; Morozov, S. V.; Jiang, D.; Zhang, Y.; Dubonos, S. V.; Grigorieva, I. V.; Firsov, A. A., Science 2004, 306, 666−669.

19. Large-area ultrathin films of reduced graphene oxide as a transparent and flexible electronic material: G. Eda, G. Fanchini, M. Chhowalla, Nature Nanotechnology, vol. 3, no. 5, pp. 270–274,2008.

20. The rise of graphene: A.K.Geim, K.S.Novoselov, Nature Materials,vol.6,no.3,pp.183–191,2007.

21. Synthesis of graphene-based nanosheets via chemical reduction of exfoliated graphite oxide: S. Stankovich, D. A. Dikin, R. D. Piner et al., vol.45,no.7,pp.1558–1565,2007.

22. Honeycomb Carbon: A Review of Graphene: M. J. Allen, V. C. Tung and R. B. Kaner, Chem. Rev., 2010, 110, 132.

23.Graphene: Status and ProspectsA. K. Geim, Science, 2009, 324, 1530.

24. Large-Area Synthesis of High-Quality and Uniform Graphene Films on Copper Foils: Xuesong Li, Weiwei Cai, Jinho An, Seyoung Kim, Junghyo Nah, Dongxing Yang, Richard Piner, Aruna Velamakanni, Inhwa Jung, Emanuel Tutuc, Sanjay K. Banerjee, Luigi Colombo, Rodney S. Ruoff, Science, 2009, 324, 1312.

25. Large-scale pattern growth of graphene films for stretchable transparent electrodes:K. S. Kim, Y. Zhao, H. Jang, S. Y. Lee, J. M. Kim, K. S. Kim, J. H. Ahn, P. Kim, J. Y. Choi and B. H. Hong, Nature, 2009, 457, 706.

26. Graphene: The New Two-Dimensional Nanomaterial: C. N. R. Rao, A. K. Sood, K. S. Subrahmanyam and A. Govindaraj, Angew. Chem., Int. Ed., 2009, 48, 7752.

27. Graphene based new energy materials: Y. Q. Sun, Q. O. Wu, G. Q. Shi, Energy Environ. Sci., 2011, 4, 1113.

28. Functional Composite Materials Based on Chemically Converted Graphene: H. Bai, C. Li, G. Q. Shi, Adv. Mater., 2011, 23, 1089.

29. Improved Synthesis of Graphene Oxide: Daniela C. Marcano, Dmitry V. Kosynkin, Jacob M. Berlin, Alexander Sinitskii, Zhengzong Sun, Alexander Slesarev, Lawrence B. Alemany, Wei Lu, James M. Tour VOL. 4 ▪ NO. 8 ▪ 4806–4814 ▪ 2010 NANO.

30. A brief review of graphene–metal oxide composites synthesis and applications in photocatalysis: Changyuan Hua, Tiewen Lua, Fei Chena Rongbin Zhangc, Journal of the Chinese Advanced Materials Society, 2013 Vol. 1, No. 1, 21–39, http://dx.doi.org/10.1080/22243682.2013.771917.

31. Chemical methods for the production of graphenes: S. Park, R. S. Ruoff, Nat. Nanotechnol., 2009, 4, 217.

32. Graphene-based composite materials: S. Stankovich, D. A. Dikin, G. H. B. Dommett, K. M. Kohlhaas, E. J. Zimney, E. A. Stach, R. D. Piner, S. T. Nguyen, R. S. Ruoff, Nature, 2006, 442, 282.

33. Biocompatibility of Graphene Oxide: K. Wang, J. Ruan, H. Song, J. Zhang, Y. Wo, S. Guo, D. Cui, Nanoscale Res. Lett., 2011, 6, 8.

34. TiO_2-decorated graphenes as efficient photoswitches with high oxygen sensitivity: Q. Wang, X. Guo, L. Cai, Y. Cao, L. Gan, S. Liu, Z. Wang, H. Zhang, L. Li, Chem. Sci., 2011, DOI: 10.1039/c1sc00344e.

35. Biocompatible, Robust Free-Standing Paper Composed of a TWEEN/Graphene Composite: S. Park, N. Mohanty, J. W. Suk, A. Nagaraja, J. An, R. D. Piner, W. Cai, D. R. Dreyer, V. Berry, R. S. Ruoff, Adv. Mater., 2010, 22, 1736.

36. Nano platforms for targeted molecular imaging in living subjects: W. B. Cai, X. Y. Chen, Small, 2007, 3, 1840.

37. Wrapping Bacteria by Graphene Nanosheets for Isolation from Environment, Reactivation by Sonication, and Inactivation by Near-Infrared Irradiation: O. Akhavan, E. Ghaderi, A. Esfandiar, J. Phys. Chem. B, 2011, 115, 6279.

38. Improving the photocatalytic performanceofgraphene-TiO2nanocomposites via a combined strategy of decreasing defects of graphene and increasing interfacial contact: Y. Zhang, N. Zhang, Z. R. Tang, Y. J. Xu, Physical Chemistry Chemical Physics,vol.14,no.25,pp.9167–9175,2012.

39. Assembly of CdS nano particles on the two-dimensional graphene scaffold as visible-light-driven photocatalyst for selective organic transformation under ambient conditions: N.Zhang, Y.Zhang, X.Pan, X.Fu, S.Liu, Y.J.Xu, Journal of Physical Chemistry C,vol.115,no.47,pp.23501–23511,2011.

40. Engineering the unique 2D mat of graphene to achieve graphene-TiO2 nano composite for photocatalytic selective transformation: what advantage does graphene have over its forebear carbon nanotube: Y. Zhang, Z. R. Tang, X. Fu, Y. J. Xu, "ACSNano,vol.5,no.9,pp.7426–7435,2011.

41. TiO_2-graphene nano composites for gas-phase photocatalytic degradation of volatile aromatic pollutant: is TiO2-graphene truly different from other TiO_2-carbon composite materials: Y. Zhang, Z. R. Tang, X. Z. Fu, Y. J. Xu, ACSNano,vol. 4,no.12,pp.7303–7314,2010.

42. Recyclable Graphene Oxide-Supported Titanium Dioxide Photocatalysts with Tunable Properties: Stuart Linley, YingYing Liu, Carol J. Ptacek, David W. Blowes, Frank X. Gu, dx.doi.org/10.1021/am4039272 | ACS Appl. Mater. Interfaces 2014, 6, 4658−4668.

43. P25-graphene composite as a high performance photocatalyst: Zhang, H., Lv, X.; Li, Y.; Wang, Y.; Li, ACS Nano 2010, 4, 380−386.

44. Hierarchically ordered macro−mesoporous TiO2−graphene composite films: Improved mass transfer, reduced charge recombination and their enhanced photocatalytic activities: Du, J.; Lai, X.; Yang, N.; Zhai, J.; Kisailus, D.; Su, F.; Wang, D.;Jiang, L.ACS Nano 2011, 5,590−596.

45. TiO_2 nano crystals grown on graphene as advanced photocatalytic hybrid materials: Y.Y. Liang, H.L. Wang, H.S. Casalongue, Z. Chen, H.J. Dai, Nano Res. 3 (2010) 701–705.

46. Synthesis of visible light responsive graphene oxide/TiO_2 composites with p/n hetero junction: C. Chen, W. Cai, M. Long, B. Zhou, Y. Wu, D. Wu, Y. Feng, ACS Nano 4 (2010) 6425–6432.

47. Enhanced cyclic performance and lithium storage capacity of SnO_2/graphene nano porous electrodes with three-dimensionally delaminated flexible structure: Paek S-M, Yoo E, Honma I. Nano Lett. 2009;9:72.

48. TiO_2-graphene nanocomposites. UV-assisted photocatalytic reduction of graphene oxide: Williams G, Seger B, Kamat PV. ACS Nano. 2008;2:1487.

49. Du J, Lai XY, Yang NL, Zhai J, Kisailus D, Su FB, Wang D, Jiang L. Hierarchically ordered macro-mesoporous TiO2-graphene composite films: Improved mass transfer, reduced charge recombination, and their enhanced photocatalytic activities. ACS Nano. 2011;5:590.

50. Synthesis of reduced graphene oxide anatase TiO_2 nano composite and its improved photo-induced charge transfer properties: P.Wang,Y.M.Zhai,D.J.Wang,S.J.Dong, , Nanoscale 3(2011) 1640–1645.

51. Sol−Gel Synthesis and Hydrothermal Processing of Anatase and Rutile Titania Nanocrystals: Wang, C.-C.; Ying, J. Y. Chem. Mater. 1999, 11, 3113−3120.
52. Development of novel TiO_2 sol–gel-derived composite and its photocatalytic activities for trichloroethylene oxidation: Keshmiri, M.; Mohseni, M.; Troczynski, T. Appl. Catal., B 2004, 53, 209−219.

53 Preparation of Graphitic Oxide: William S. Hummers Jr., Richard E. Offeman, J. Am. Chem. Soc. 80 (1958) 1339.
54. Graphite oxide/poly(methyl methacrylate) nano composites prepared by a novel method utilizing macro azo initiator: J.Y. Jang, M.S. Kim, H.M. Jeong, C.M. Shin, Compos. Sci. Technol. 69 (2009) 186–191.
55. Photo-degradation of methylene blue by multi-walled carbon nanotubes/TiO_2 composites: G. Jiang, X. Zheng, Y. Wang, T. Li, X. Sun, Powder Technol. 207 (2011) 465–469.

56. The role of graphene oxide content on the adsorption-enhanced photocatalysis of titanium dioxide/graphene oxide composites: T.-D. Nguyen-Phan, V.H. Pham, E.W. Shin, H.-D. Pham, S. Kim, J.S. Chung, E.J. Kim, S.H. Hur, Chem. Eng. J.170 (2011) 226–232.
57. Nano composites of TiO_2 and reduced graphene oxide as efficient photocatalysts for hydrogen evolution: W.Fan, Q.Lai,Q.Zhang, Y.Wang, J.Phys.Chem.C115(2011)10694–10701.

58. TiO_2 nano particles assembled on graphene oxide nano sheets with high photocatalytic activity for removal of pollutants: G.Jiang, Z.Lin, C.Chen, L.Zhu, Q.Chang, N.Wang, W.Wei H.Tang, Carbon49 (2011)2693–2701.

59. Daylight photocatalysis by carbon-modified titanium dioxide: S. Sakthivel, H. Kisch Angew. Chem. Int. Ed. 42 (2003) 4908–4911.

60. Is the band gap of pristine TiO_2 narrowed by anion- and cation doping of titanium dioxide in second-generation photocatalysts?: N. Serpone, J Phys. Chem. B. 110 (2006) 24287–24293.

61. Daylight Photocatalysis by Carbon-Modified
Titanium Dioxide**
Shanmugasundaram Sakthivel and Horst Kisch* Angew. Chem. Int. Ed. 2003, 42, 4908 –4911

62. XPS study of the halogenation of carbon black—Part 2. Chlorination: E. Papirer, R. Lacroix, J.-B. Donnet, G. Nanse, P. Fioux, Carbon 1995, 33, 63.
63. Effect of glucose on photocatalytic decolorization of dyes by TiO_2: Konitou K.; Maeda S.; Hongyou S.; Mishima K., J. Chem. Eng. 80 (2002) 208.
64. http://www.redwop.com